Carcinogenesis, 2022, **43**, 150–159
https://doi.org/10.1093/carcin/bgab124
Advance access publication 18 December 2021
Original Article

OXFORD

Original Article

The miR-345-3p/PPP2CA signaling axis promotes proliferation and invasion of breast cancer cells

Qian Zeng[1,†], Fangfang Jin[1,†], Husun Qian[1], Hongling Chen[1], Yange Wang[1], Dian Zhang[1], Yu Wei[1], Tingmei Chen[1], Bianqin Guo[2,*] and Chengsen Chai[1,*]

[1]Key Laboratory of Clinical Laboratory Diagnostics (Ministry of Education), College of Laboratory Medicine, Chongqing Medical University, Chongqing 400016, P.R. China
[2]Department of Clinical Laboratory, Chongqing University Cancer Hospital, Chongqing 40030, P.R. China

[†]These authors contributed equally to this work.
*To whom correspondence should be addressed; Tel: +86-023-68485216; Fax: 0086-023-68485938;
Email: chengsenchai@cqmu.edu.cn
Correspondence may also be addressed to Bianqin Guo. Tel: +86-13512388623; Fax: 0086-023-65310296;
Email: 178098941@qq.com

Abstract

Breast cancer is the most common malignancy among women worldwide. Functional studies have demonstrated that miRNA dysregulation in many cases of cancer, in which miRNAs act as either oncogenes or tumor suppressor. Here we report that miR-345-3p is generally upregulated in breast cancer tissues and breast cancer cell lines. Overexpression and inhibition of miR-345-3p revealed its capacity in regulating proliferation and invasion of breast cancer cells. Further research identified protein phosphatase 2 catalytic subunit alpha (PPP2CA), a suppressor of AKT phosphorylation, as a candidate target of miR-345-3p. *In vitro*, miR-345-3p mimics promoted AKT phosphorylation by targeting its negative regulator, PPP2CA. Blocking miR-345-3p relieved its inhibition of PPP2CA, which attenuated PI3K-AKT signaling pathway. *In vivo*, inhibiting miR-345-3p by miR-345-3p-inhibition lentivirus suppressed tumor growth and invasiveness in mice. Together, the miR-345-3p/PPP2CA signaling axis exhibits tumor-promoting functions by regulating proliferation and invasion of breast cancer cells. These data provide a clue to novel therapeutic approaches for breast cancer.

Abbreviations: FBS, fetal bovine serum; FISH, fluorescence *in situ* hybridization; miRNA, microRNAs; STR, short tandem repeat.

Introduction

Breast cancer is the most common cancer among women worldwide, accounting for approximately 30% of all new cases in female cancers (1). Despite significant improvements in diagnosis and treatment modalities, breast cancer remains the second leading cause of cancer-related death for women globally, accounting for approximately 15% of all death cases in female cancers (1,2). The high rates of cancer-related death are majorly linked to metastasis and recurrence (3–6), which hinders satisfactory of treatment. Therefore, identifying molecular mechanism involved in breast cancer initiation and progression is urgently needed to find effective targets and treat breast cancer.

MicroRNAs (miRNAs) are a class of small non-coding RNA molecules with a length of approximately 22 nucleotides, which play a regulatory role in gene expression and a range of biological functions, including cell differentiation, proliferation and survival by binding to their complementary target mRNAs, resulting in mRNA post-translation repression or degradation (7,8). Many miRNAs are evolutionarily conserved across evolution (9,10), which implies that these miRNAs direct essential processes during development. There is considerable evidence to indicate that miRNAs are involved in the development and progression of cancer (11–14). In different types of cancers, miRNAs can function as either oncogenes or tumor suppressor through expression regulation of their target genes. Importantly, cancer-associated microRNA can be detected in biological fluids, such as urine, saliva and serum, allowing less-invasive monitoring and diagnosis (15–17). A previous study found that miR-345-3p regulated endothelial function and lipid homeostasis through the TAK1/p38/NF-κB pathway (18). Another report demonstrated the protective function of miR-345-3p in patients with GDM (19). However, the role of miR-345-3p in breast cancer has not yet been investigated.

In this study, we confirmed that miR-345-3p was upregulated in breast cancer tissues and breast cancer cell lines. Moreover, elevated miR-345-3p promotes proliferation and invasion of breast cancer cells by downregulating PPP2CA, a well-known suppressor of AKT phosphorylation, thereby activating PI3K-AKT signaling pathway. Furthermore, both *in vitro* and *in vivo* studies demonstrated that knockdown of miR-345-3p remarkably attenuated the proliferation and invasion of breast cancer cells. Collectively, our findings revealed a biological mechanism by which

Received: October 14, 2021; Revised: November 27 2021; Accepted: December 10, 2021

miR-345-3p contributes to breast cancer proliferation and invasion, providing a clue to novel targets for therapeutic strategies.

Materials and methods

Cell lines and culture

The MDA-MB-231 and MCF-7 cells were purchased from Kunming Institute of Zoology, Chinese Academy of Sciences. The SK-BR3 and MCF-10A cells were purchased from Procell (Wuhan, China). T47D cells were purchased from National Collection of Authenticated Cell Cultures (Shanghai, China). All cells were authenticated using short tandem repeat (STR) profiling at the time of purchase (2021). MCF-7, T47D and SK-BR3 cells were cultured in Dulbecco's modified Eagle's medium (DMEM; Gibco, USA) supplemented with 10% fetal bovine serum (FBS) and 1% penicillin/streptomycin. MDA-MB-231 cells were cultured in DMEM/F-12 (1:1) medium (BasalMedia, China) supplemented with 10% fetal bovine serum (FBS; Gibco, USA) and 1% penicillin/streptomycin. MCF-10A cells were cultured in MCF-10A special medium (Procell Life Science &Technology, China). All cells were cultured in a humidified atmosphere of 5% CO2 at 37°C according to ATCC standard protocols.

RNA extraction and quantitative real-time RT-PCR

Total RNA was extracted using Trizol reagent (Takara, Japan) according to the manufacturer's instructions. For reverse transcription of RNA, 1 μg of total RNA was reverse-transcribed using miRNA ALL-In-One cDNA synthesis kit (abm, Canada) and PrimeScript RT reagent kit (TaKaRa, Japan). Quantitative PCR was performed using EvaGreeen miRNA qPCR MaterMix (abm, Canada) and SYBR Premix Ex Taq II (TaKaRa, Japan). U6 and β-actin served as the internal control to quantify the relative expression of miRNA and mRNA. Primer sequences for the detected genes were listed in Supplementary Table S1, available at *Carcinogenesis* online.

Clinical breast tumor samples

Human breast cancer tissue and its paired adjacent normal tissues are from the Department of Pathology, the First Affiliated Hospital of Chongqing Medical University. According to the patients' medical records, the tissues from patients with breast cancer without previous radiotherapy or chemotherapy are selected for experiment. Tissues were fixed in 10% formalin for 24 h at room temperature, embedded in paraffin as for routine histology, sectioned at 4 μm thickness and dried thoroughly at 50°C overnight for subsequence analysis.

Fluorescence *in situ* hybridization

MicroRNA fluorescence *in situ* hybridization (FISH) probe and FISH kit (GenePharma, China) were used for detection of miR-345-3p in human breast cancer tissues and paired normal mammary tissues. FISH was performed according to the manufacturer's protocols. Briefly, after dewaxing, the paraffin sections were digested with proteinase K and denatured at 78°C for 8 min, and then hybridized with the pre-denatured miR-345-3p FISH Probe at 37°C overnight. The nucleus was stained with DAPI. The picture was captured by a confocal microscope (Leica TCS SP8, Germany).

Cell transfection, lentivirus infection and plasmids constructs

The GV272-PPP2CA-3′-UTR-WT plasmid which contains the putative miR-345-3p-binding sites and GV272-PPP2CA-3′-UTR-MUT plasmid whose putative miR-345-3p-binding sites was mutated were acquired from Genechem (Shanghai, China). All constructs were confirmed by DNA sequencing. To establish the stably interfered cells, cells were transfected with the hsa-miR-345-3p-inhibition lentivirus (Genechem, Shanghai, China) and control lentivirus (Genechem, Shanghai, China) for 48 h, and then undergoing selection with puromycin for 2 weeks. The miR-345-3p mimics/inhibitor and the negative control (NC) were purchased from GenePharma (Shanghai, China). PPP2CA siRNA was synthesized from Labcell (Chongqing, China). The sequences of PPP2CA siRNA were provided in Supplementary Table S1, available at *Carcinogenesis* online. Lipofectamine 2000 (Invitrogen, Grand Island, NY, USA) was used for transfection following the manufacturer's instructions.

Measurement of cell growth

Cell Counting Kit-8 (CCK-8) (MCE, China) assay was used to determine viability of the indicated cells. Briefly, the cells of each group were transfected with corresponding reagents, and negative control (NC) served as the control. After 48 h of treatment, cell suspension was seeded in 96-well plates at a density of 5×10^3 cells/ well. After cultured for 24 h, 48 h, and 72 h, respectively, cells were incubated in 10% Cell Counting Kit-8 (CCK-8) at 37°C for 1.5 h. The optical density (OD) value at 450 nm was read in digital spectrophotometer. Each experiment was repeated three times.

Wound-healing assay

Cells were planted into 6-well plate. Cells in different groups were transfected with indicated reagents when the cell confluence reaching 60%-80%. A pipette tip was used to make a scratch in the monolayer, and removing floating cells with PBS. The remaining adherent cells were culture in serum-free medium to satisfy cell growth and wound healing. After cultured for 0 h, 12 h, 24 h, and 36 h, respectively, images were taken with the phase contrast microscope (Olympus, Tokyo, Japan).

Transwell assay

The Matrigel (1:8 dilution; BD Bioscience) was diluted with serum-free medium, and the chamber containing 100 μl of diluted Matrigel was incubated at 37°C for 1.5 h. The transwell chamber was placed on a 24-well plate whose lower chamber containing 500 μl medium with 10% FBS according to manufacturer's protocols. The treated cells were washed with PBS and resuspended in serum-free medium, and 200 μl serum-free medium containing 2×10^4–3×10^4 cells was added to each chamber. After cultured for 48 h, the invading cells transferred to the lower layer were fixed, stained with crystal violet, and imaged under microscope.

Western blotting

Protein was extracted from the indicated cells using RIPA lysis buffer (Beyotime, China) supplemented with protease inhibitors PMSF (Beyotime, China). The protein concentration was measured using bicinchoninic acid (BCA) protein assay kit (Beyotime, China). The lysates isolated from indicated

cells were separated by 10% SDS–polyacrylamide gels and immunoblotted with appropriate antibodies. The specific primary antibodies against E-cadherin (20874-1-AP, Proteintech; 1:1000), N-cadherin (22018-1-AP, Proteintech; 1:1000), MMP2 (66366-1-lg, Proteintech; 1:1000), Snail (3895S, Cell Signaling Technology; 1:1000), c-Myc (5605T, Cell Signaling Technology; 1:1000), CyclinD1 (01435a, wanleibio; 1:1000), Bcl-2 (BF9103, Affinity; 1:1000), Bax (2772T, Cell Signaling Technology; 1:1000), α-Tubulin (66031-1-lg, Proteintech; 1:1000), PPP2CA (AF4753, Affinity; 1:1000), p-Akt (4060S, Cell Signaling Technology, 1:1000), AKT (C67E7, Cell Signaling Technology, 1:1000) were used and incubated at 4°C overnight. The membranes were then incubated with the peroxidase conjugated secondary antibody (Bioworld, 1:10000) for 1 h at room temperature. The proteins were visualized by enhanced chemiluminescence assay (Millipore Corporation).

Luciferase reporter assay

Cells cultured in 24-well plates were co-transfected with 1 μg of wide-type or mutated PPP2CA 3′UTR constructs, and NC or miR-345-3p mimics using Lipofectamine 2000 (Invitrogen, Grand Island, NY, USA) according to the manufacturer's instruction. Luciferase activity was measured 48 h after transfection using the Luc-Pair™ Duo-Luciferase HS Assay Kit (GeneCopoeia, USA). Firefly luciferase activity was normalized to Renilla luciferase activity for each sample.

Xenograft mouse model

Animal experiments were conducted in accordance with standard guidelines on animal care approved by the Chongqing Medical University Experimental Animal Management Committee. Breast cancer cells (1×10^6 cells in 150 μl PBS) were transduced with hsa-miR-345-3p-inhibition lentiviral vector (experimental group) or with control vector (control group), and injected subcutaneously into BALB/c-nude mice aged 3–4 weeks. Three mice were used in each group. Tumor volumes were measured by caliper every week and calculated based on the following formula: tumor volume (mm^3) = 1/2 length × $width^2$. At the end of animal experiments, mice were sacrificed. Tumor tissue were isolated, weighed, photographed, and used for further immunohistochemistry (IHC) staining to detect associated protein expression.

Immunohistochemistry

Paraffin-embedded samples from mice were sectioned at 4 μm thickness, and then deparaffinied in xylene, rehydrated through a graded alcohol series and retrieved in 10 mM sodium citrate buffer (pH 6.0). Then the slides were incubated with hydrogen peroxide to block endogenous peroxidase activity, followed by incubation in 10% goat serum to block nonspecific binding. The tissue sections were incubated with primary antibodies at 4 °C overnight and subsequently followed by HRP secondary antibody at room temperature for 30 min, then stained with diaminobenizidine. The specific primary antibodies against PPP2CA (2259T, Cell Signaling Technology, 1:25), Ki67 (GB111499, Servicebio, 1:100), E-cadherin (GB12082, Servicebio, 1:100), N-cadherin (22018-1-AP, Proteintech; 1:100) were used. DAB (SA-HRP) Tunel Cell Apoptosis Detection Kit (G1507-100T, Servicebio) were used for detection of cell apoptosis in the tissue sections. IHC stainings were visualized and imaged with the microscopy (Nikon ECLIPSE Ti-s, Japan).

Statistical analysis

The SPSS 20.0 statistical software and GraphPad Prism 8.0 were used for statistical analysis. The results were presented as means ± SD. Student's *t*-test and one-way analysis of variance (ANOVA) were used to evaluate the significance of two groups and multiple groups respectively. Each experiment was performed independently at least three times. Differences with P-value < 0.05 were considered statistically significant.

Results

miR-345-3p is upregulated in breast cancer tissues and breast cancer cell lines, and positively correlated with poor prognosis

To investigate the role of miR-345-3p in breast cancer pathogenesis, we firstly determined the expression level of miR-345-3p by taking advantage of the TCGA database. As shown in Figure 1A, miR-345-3p expression was significantly elevated in breast cancer tissues compared with their adjacent normal breast tissues. We next performed further verification in the cell lines. MCF-7, T47D, SKBR3, MDA-MB-231 cells and normal mammary epithelial cells MCF-10A were used. As shown in Figure 1B, compared to normal breast cells, the increased miR-345-3p expression was detected in several breast cancer cells. Furthermore, the expression of miR-345-3p was obviously upregulated in highly metastatic MDA-MB-231 and SKBR3 cells in comparison with lowly metastatic MCF-7 and T47D cells. These results suggest that miR-345-3p expression may be positively correlated with the metastatic ability of breast cancer cells. We observed that miR-345-3p expression was elevated in tumor tissues by using FISH, whereas little fluorescence signal was detected in their corresponding normal tissues (Figure 1C). In addition, Kaplan-Meier plot demonstrated that breast cancer patients with higher expression of miR-345-3p had worse prognosis from TCGA database (Figure 1D; Supplementary Figures S4–S6). These data indicated that increased miR-345-3p expression in breast cancer was positively correlated with poor prognosis.

miR-345-3p promotes proliferation and invasion of breast cancer cells

To study the contribution of miR-345-3p to proliferation and invasion of breast cancer cells, we ectopically expressed miR-345-3p in MCF-7 cells which have low endogenous miR-345-3p expression, and knocked down miR-345-3p expression in MDA-MB-231 cells with high miR-345-3p level. MCF-7 and MDA-MB-231 cells were transfected with miR-345-3p mimics and miR-345-3p inhibitors respectively, and the transfection efficiency was verified by qRT-PCR (Figure 2A). The wound-healing assay revealed that compared to control cells, overexpression of miR-345-3p significantly promoted the migration of MCF-7 cells. In contrast, knockdown of miR-345-3p with the oligonucleotide inhibitor remarkably attenuated the migration of MDA-MB-231 cells (Figure 2B). Meanwhile, the capacity of proliferation in breast cancer cells was detected by CCK-8 assay. As demonstrated in Figure 2C, miR-345-3p mimics treatment resulted in remarkable increase in proliferation of MCF-7 cells. On the contrary, inhibition of miR-345-3p suppressed the proliferation capacity of

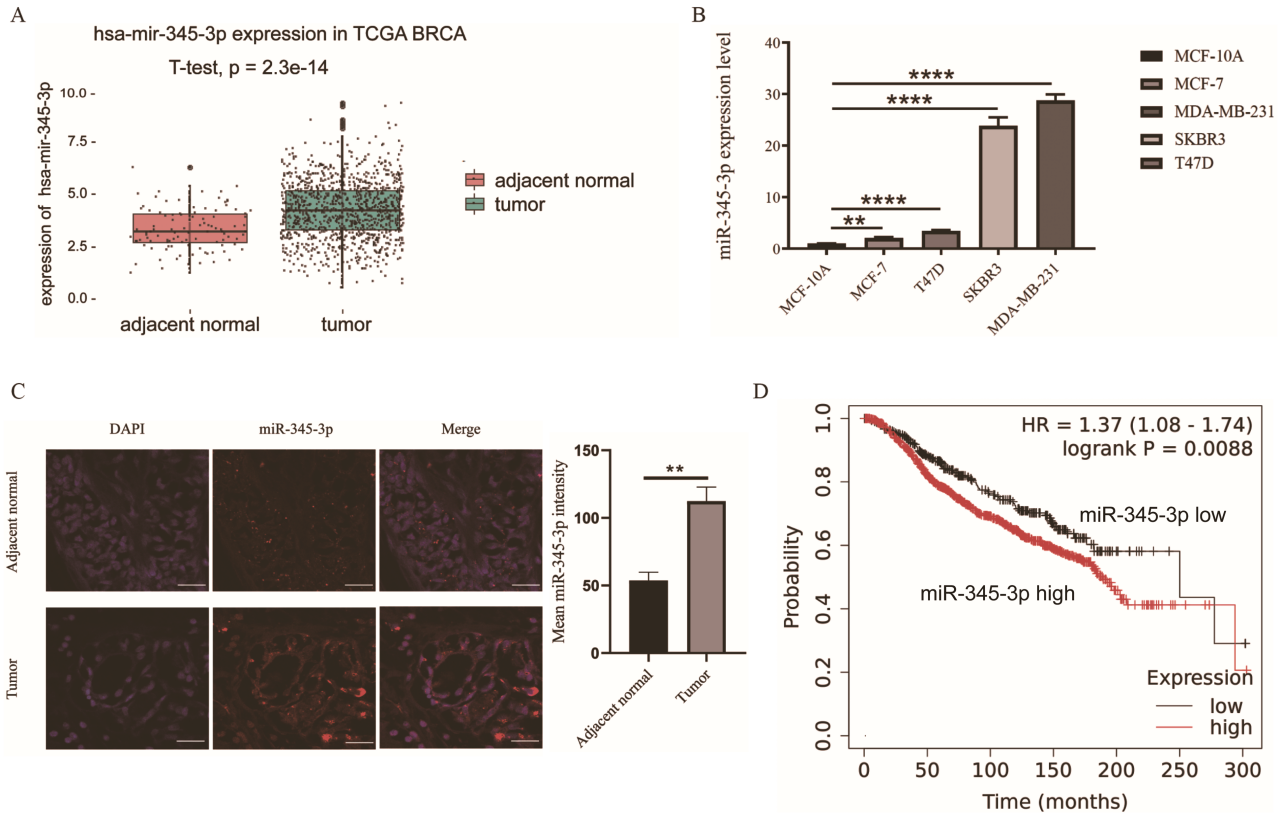

Figure 1. The upregulation of miR-345-3p in breast cancer cell lines and tissues is positively correlated with poor prognosis. A, miR-345-3p expression was elevated in breast cancer tissues compared with their adjacent normal breast tissues in TCGA database. B, High miR-345-3p level was detected in breast cancer cell lines (MCF-7, T47D, SKBR3, MDA-MB-231) compared with human normal mammary epithelial cells (MCF-10A) by using qRT-PCR analysis. U6 RNA served as the internal control. C, miR-345-3p expression was visualized in human breast cancer tissues and their adjacent normal breast tissues by FISH assays. Representative images of miR-345-3p in tissues are shown. DAPI: 4′,6-diamidino-2-phenylindole; the used probe: miR-345-3p. Scale bar, 50 μm. D, High level of miR-345-3p was positively correlated with poor prognosis. All data are presented as the mean ± SD of triplicate experiments. The *P*-values < 0.05 were considered statistically significant. **P* < 0.05, ***P* < 0.01, ****P* < 0.001, *****P* < 0.0001.

MDA-MB-231 cells (Figure 2C). In accordance with these results, the Transwell invasion assay showed that miR-345-3p could increase the invasion ability of MCF-7 cells significantly, whereas control cells barely penetrated matrigel (Figure 2D). However, knockdown of miR-345-3p significantly attenuated invasiveness in MDA-MB-231 cells (Figure 2D). Furthermore, we measured the expression level of several protein markers involved in epithelial-mesenchymal transition (EMT) process. As expected, overexpression of miR-345-3p significantly upregulated the expression of proteins positively related to cell invasion such as N-cadherin, MMP2, snail in comparison with their control cells, whereas the expression of epithelial marker E-cadherin was notably decreased under miR-345-3p mimics treatment (Figure 2E). In contrast, compared to the control of inhibitors NC cells, high E-cadherin expression and low N-cadherin, MMP2, snail expression were detected in MDA-MB-231 cells transfected with miR-345-3p inhibitors (Figure 2E). To further identify the molecular mechanism of miR-345-3p on breast cancer cell proliferation, we examined the expression of several protein markers involved in cell cycle process and apoptosis. As shown in Figure 2E, there is no significant difference in c-Myc and cyclinD1 expression between control cells and cells transfected with miR-345-3p mimics or miR-345-3p inhibitors. However, overexpression of miR-345-3p upregulated expression of Bcl-2 and downregulated expression of Bax. Likewise, miR-345-3p inhibitors treatment resulted in increased expression of Bax and decreased expression of Bcl-2. To further confirm this finding, we performed TUNEL assay and flow cytometry assay. TUNEL assay revealed that miR-345-3p mimics suppressed apoptosis compared with the control in MCF-7 cells (Supplementary Figure S1A, available at *Carcinogenesis* online). On the contrary, miR-345-3p inhibitors markedly promoted apoptosis (Supplementary Figure S1B, available at *Carcinogenesis* online). However, neither miR-345-3p mimics nor miR-345-3p inhibitors could regulate cell cycle (Supplementary Figure S1C and D, available at *Carcinogenesis* online). Taken together, these results suggested that miR-345-3p promoted proliferation and invasion of breast cancer cells and miR-345-3p affected cell proliferation by regulating apoptosis rather than cell cycle.

miR-345-3p mediates proliferation and invasion of breast cancer cells by regulating its downstream targets PPP2CA

To further elucidate the molecular mechanisms how miR-345-3p could participate in proliferation and invasion of breast cancer cells, we sought to identify downstream effectors of miR-345-3p using bioinformatics prediction websites miRDB, Targetscan and miRtarbase. A total of 22 genes were found in all the three databases (Figure 3A, Supplementary Table S2, available at *Carcinogenesis* online). Moreover, pathways involved in these 22 genes were

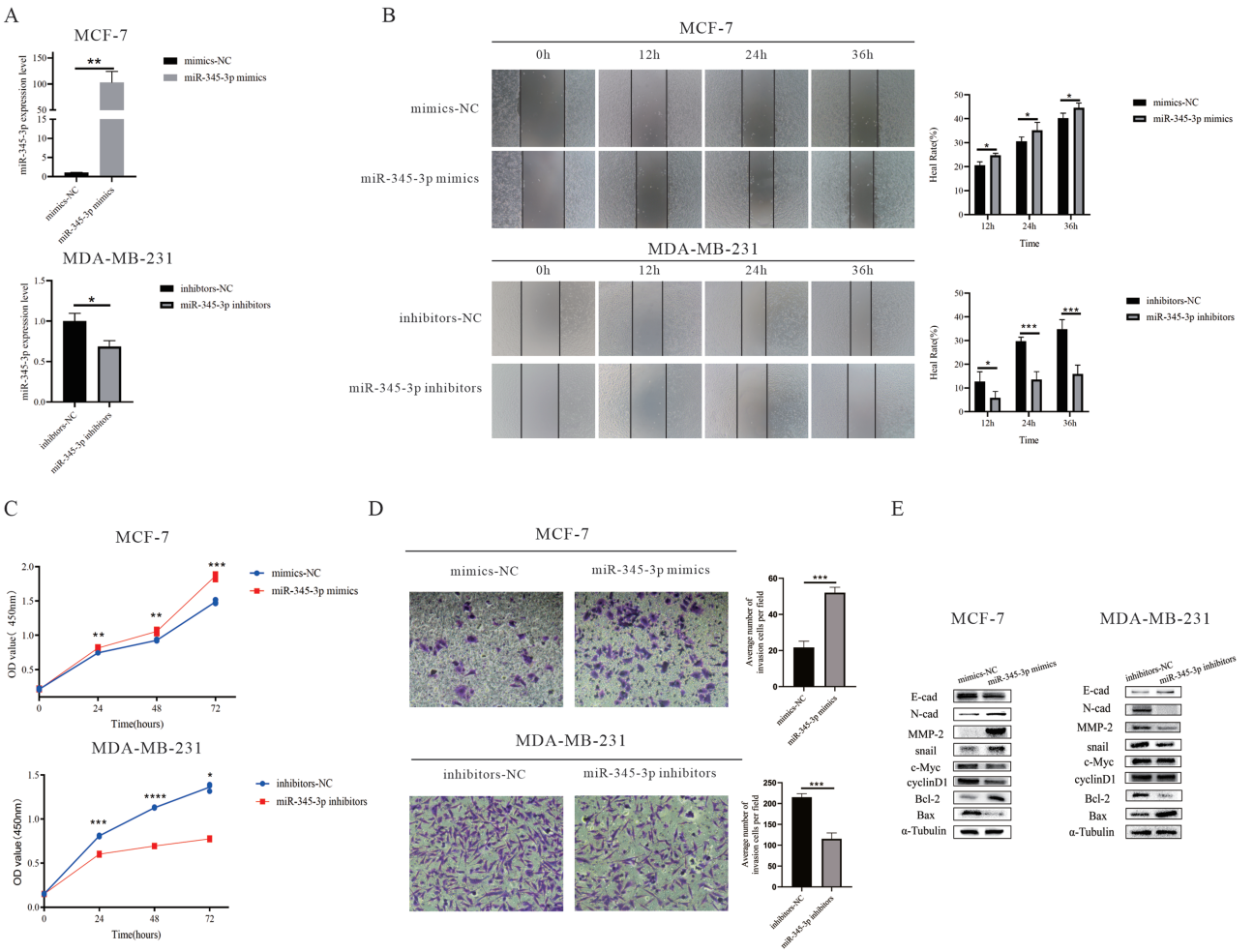

Figure 2. MiR-345-3p promotes proliferation and invasion of breast cancer cells. A, The transfection efficiency was verified by qRT-PCR. Twenty-four hours after transfection, the expression level of miR-345-3p was detected by q-PCR. U6 RNA served as the internal control. B, The effect of miR-345-3p on cell migration was examined by wound-healing assay. The wound-healing efficacy were tested in miR-345-3p-knocked down cells, miR-345-3p-overexpression cells and their control cells at 12 h, 24 h, 36 h. C, The effect of miR-345-3p on cell viability was analyzed by CCK-8 assay. Relative cell viability of MCF-7 and MDA-MB-231 cells after transfection with miR-345-3p mimics and miR-345-3p inhibitors respectively were detected by CCK-8 assay at 24 h, 48 h, 72 h. D, The effect of miR-345-3p on cell invasion ability was measured by the transwell assay. E, The effect of miR-345-3p on EMT was detected by Western blot assay. Forty-eight hours after treatment, cell lysates were prepared and measured by Western blotting with the indicated antibodies. α-Tubulin was used as a loading control. All data are presented as the mean ± SD of triplicate experiments. The *P*-values < 0.05 were considered statistically significant. **P* < 0.05, ***P* < 0.01, ****P* < 0.001, *****P* < 0.0001.

analyzed with KOBAS 3.0. The results indicated that 5 signal pathways were predicted to be involved ($P < 0.05$), including autophagy, PI3K-Akt signaling pathway, Sphingolipid signaling pathway, AMPK signaling pathway, and pantothenate and CoA biosynthesis (Figure 3B, Supplementary Table S3, available at *Carcinogenesis* online). Furthermore, among the prediction scores of miRDB, PPP2CA had a higher score and participated in multiple pathways involved in these common 22 genes (Supplementary Tables S2 and S3, available at *Carcinogenesis* online). Therefore, we finally identified PPP2CA as the potential downstream target of miR-345-3p. To further evaluate whether miR-345-3p directly interacted with the 3′ UTR of PPP2CA, we predicted miR-345-3p-binding site by taking advantage of web-based software TargetScan (Figure 3C). Moreover, the dual-luciferase UTR vectors carrying the wild-type 3′ UTR of PPP2CA (PPP2CA 3′ UTR WT) and the mutant 3′ UTR of PPP2CA (PPP2CA 3′ UTR MUT) in which miR-345-3p-binding site was mutated were constructed for luciferase reporter assays. MCF-7 cells were transfected with the indicated dual-luciferase vectors together with the control or with miR-345-3p mimics. As shown in Figure 3D, miR-345-3p mimics significantly decreased the luciferase activity driven by PPP2CA 3′ UTR WT. In contrast, miR-345-3p mimics had no significant effect on the luciferase activity of PPP2CA 3′ UTR MUT vector. Consistent with these observations, miR-345-3p mimics treatment obviously reduced the PPP2CA expressions at both mRNA and protein levels in MCF-7 cells (Figure 3E and F). Besides, inhibition of miR-345-3p resulted in a remarkable increase in PPP2CA at mRNA and protein levels (Figure 3E and F), hence supporting the hypothesis that PPP2CA is a direct target of miR-345-3p.

Furthermore, to study the functional roles of miR-345-3p-mediated upregulation of PPP2CA in proliferation and invasion of breast cancer cells, siRNA-mediated silencing of PPP2CA was performed in MDA-MB-231 cells (Supplementary Figure S2A, available at *Carcinogenesis* online). We then chose PPP2CA siRNA#1 for the following experiment. As shown in Figure 4A, MDA-MB-231 cells were

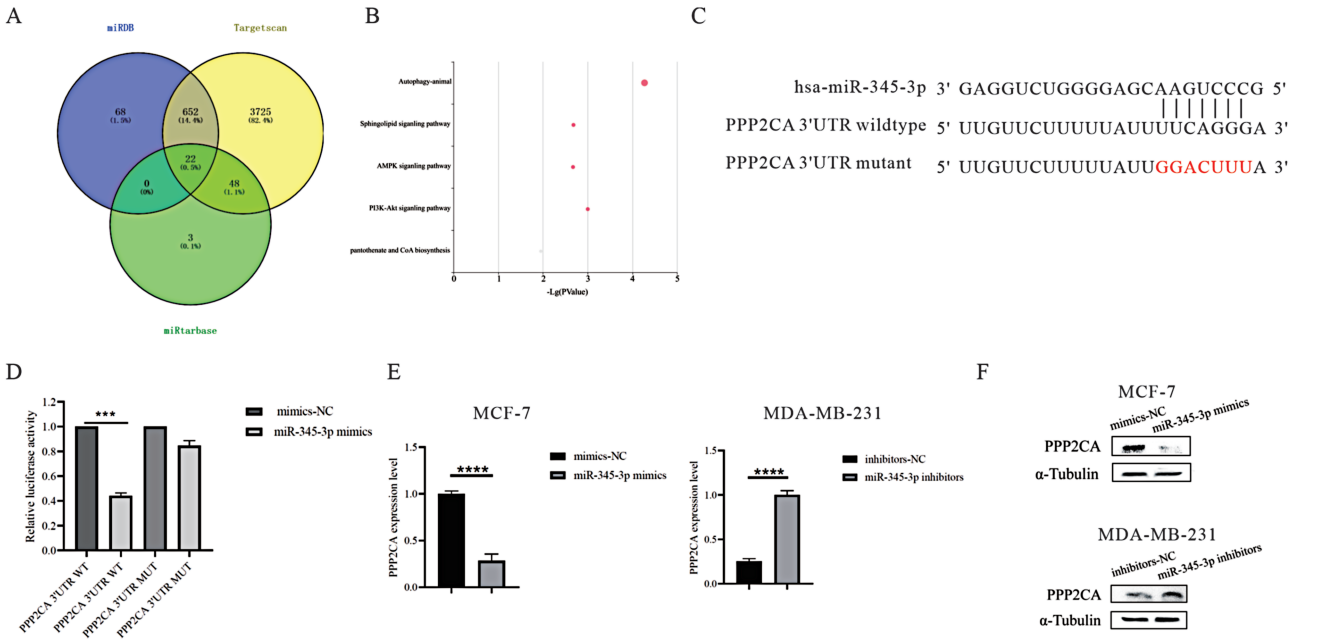

Figure 3. PPP2CA is the direct downstream targets of miR-345-3p. A, Venn diagrams represent the common potential target genes of miR-345-3p predicted by miRDB, Targetscan and miRtarbase. B, Pathways involved in these 22 genes were analyzed with KOBAS 3.0. C, A schematic diagram of the binding sequence was presented. D, Luciferase reporter assays in MCF-7 cells after co-transfection of PPP2CA wild-type or mutated 3′UTR luciferase reporter constructs together with miR-345-3p mimics or with the control miRNA. Forty-eight hours after transfection, luciferase activities were detected. E, mRNA level of PPP2CA in miR-345-3p-knocked down cells, miR-345-3p-overexpression cells and their control cells were determined by qRT-PCR. Twenty-four hours after transfection, total RNA was prepared and the expression level of miR-345-3p was detected by qRT-PCR. U6 RNA served as the internal control. F, protein level of PPP2CA in miR-345-3p-knocked down cells, miR-345-3p-overexpression cells and their control cells were determined by Western blot assay. Forty-eight hours after treatment, cell lysates were prepared and measured by western blotting with the indicated antibodies. α-Tubulin was used as a loading control. All data are presented as the mean ± SD of triplicate experiments. The *P*-values < 0.05 were considered statistically significant. **P* < 0.05, ***P* < 0.01, ****P* < 0.001, *****P* < 0.0001.

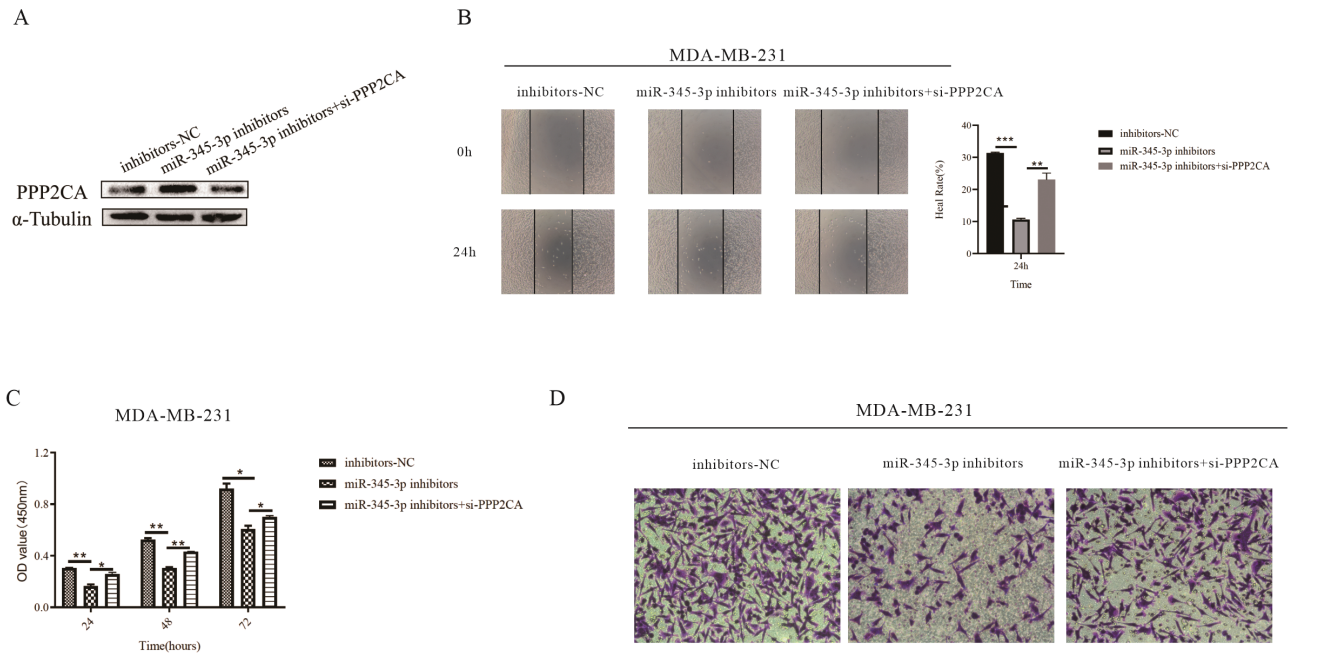

Figure 4. Silencing of PPP2CA rescued the inhibition of cell proliferation and invasion induced by miR-345-3p inhibitors. A, PPP2CA siRNA significantly decreased the expression of PPP2CA under treatment of miR-345-3p inhibitors. Forty-eight hours after treatment, cell lysates were prepared and measured by Western blotting with the indicated antibodies. α-Tubulin was used as a loading control. B, Silencing of PPP2CA abrogated the inhibition of cell migration abilities induced by miR-345-3p inhibitors. The wound-healing efficacy were tested in MDA-MB-231 cells at 24 h. C, Silencing of PPP2CA abrogated the inhibition of cell proliferation abilities induced by miR-345-3p inhibitors. Relative cell viability of MDA-MB-231 cells were detected by CCK-8 kit at 24 h, 48 h, 72 h. D, Silencing of PPP2CA abrogated the inhibition of cell invasion abilities induced by miR-345-3p inhibitors. Cells invasion ability was measured by Transwell assay. All data are presented as the mean ± SD of triplicate experiments. The *P*-values < 0.05 were considered statistically significant. **P* < 0.05, ***P* < 0.01, ****P* < 0.001, *****P* < 0.0001.

co-transfected with miR-345-3p inhibitors and PPP2CA siRNA, PPP2CA siRNA significantly decreased the expression of PPP2CA under treatment of miR-345-3p inhibitors. The wound-healing assay and CCK-8 assay revealed that silencing of PPP2CA abrogated the inhibition of cell migration and proliferation abilities induced by miR-345-3p inhibitors (Figure 4B and C). Consistently, the depletion of PPP2CA partially rescued the inhibition of cell invasion induced by miR-345-3p inhibitors (Figure 4D). In summary, these results demonstrated that PPP2CA was required at least in part for miR-345-3p-mediated proliferation and invasion of breast cancer cells.

miR-345-3p affects proliferation and invasion of breast cancer cells through regulation of PI3K-AKT signaling pathway

As mentioned above, we found that PPP2CA, a well-known suppressor of AKT phosphorylation (20), could be as a direct downstream target of miR-345-3p. Additionally, the results of enriched pathways predicted by bioinformatics websites showed that PI3K-AKT signaling pathway was exactly included. We assessed whether miR-345-3p affects proliferation and invasion of breast cancer cells through regulation of PI3K-AKT signaling pathway. MCF-7 and MDA-MB-231 cells were transfected with miR-345-3p mimics and miR-345-3p inhibitors respectively. As expected, expression of p-AKT was dramatically enhanced upon overexpression of miR-345-3p. In contrast, knockdown of miR-345-3p with the oligonucleotide inhibitor remarkably attenuated the expression level of p-AKT (Figure 5A). To understand how PI3K-AKT signaling pathway exert their functions in proliferation and invasion of breast cancer cells, Akt activator SC79 was used in MDA-MB-231 cells. The efficiency of Akt activator SC79 on cell migration and invasion ability was evaluated by wound-healing assay and transwell assay, which revealed that Akt activator SC79 abrogated the inhibition of cell migration and invasion abilities induced by miR-345-3p inhibitors (Figure 5B and D). Similarly, the Akt activator SC79 partially rescued the inhibition of cell proliferation induced by miR-345-3p inhibitors (Figure 5C). Collectively, these data suggested that PI3K-AKT signaling pathway activation was required at least in part for miR-345-3p-mediated proliferation and invasion of breast cancer cells.

Knockdown of miR-345-3p attenuates cell growth and invasiveness *in vivo*

To unravel the therapeutic role of miR-345-3p in breast cancer initiation and progression, miR-345-3p stable knockdown cells were established. The stable transfection efficiency was validated with fluorescence signal and qRT-PCR (Supplementary Figure S3A and B, available at *Carcinogenesis* online). MDA-MB-231 cells transduced with the control lentiviral vector or with miR-345-3p-inhibition lentiviral vector were subcutaneously implanted into BALB/c-nude mice. As seen in Figure 6A–C, miR-345-3p knockdown obviously suppressed tumor growth compared with the control group treated with the control lentiviral vector alone. Moreover, in agreement with our *in vitro* results, knockdown

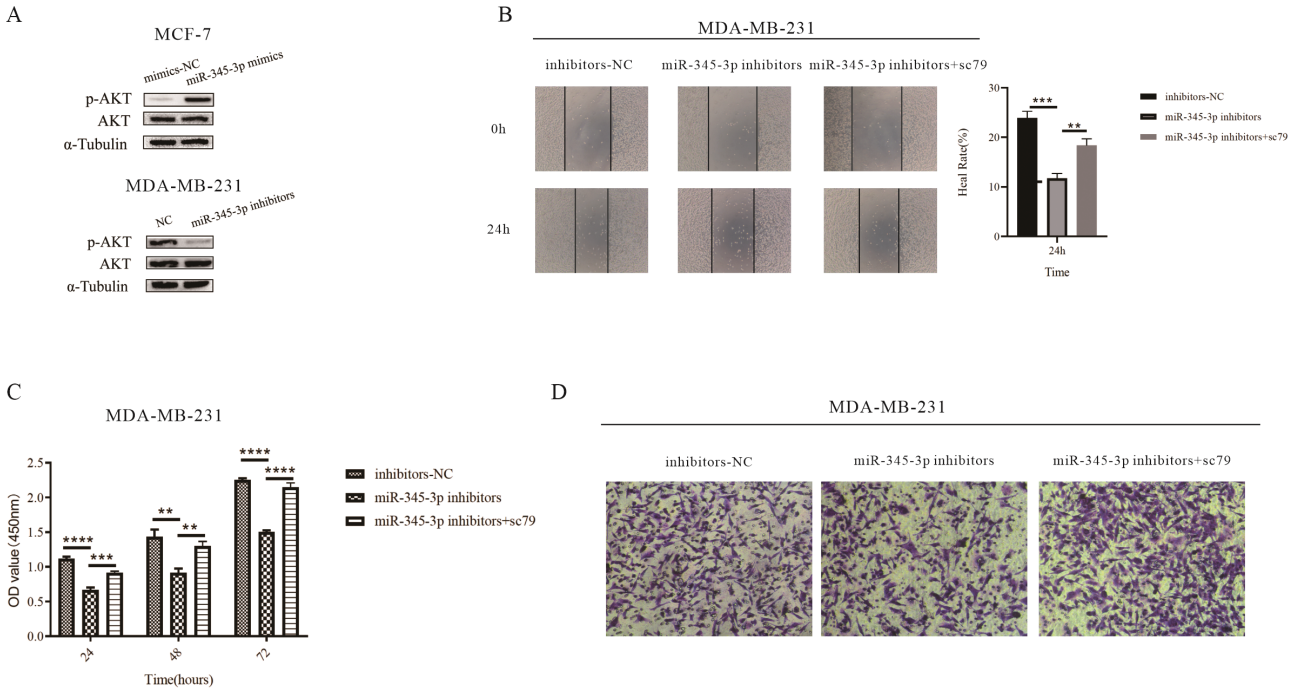

Figure 5. PI3K-AKT signaling pathway activation rescued the inhibition of cell proliferation and invasion induced by miR-345-3p inhibitors. A, p-AKT level in miR-345-3p-knocked down cells, miR-345-3p-overexpression cells and their control cells were detected by western blot assay. Forty-eight hours after treatment, cell lysates were prepared and measured by Western blotting with the indicated antibodies. α-Tubulin was used as a loading control. B, Akt activator SC79 abrogated the inhibition of cell migration abilities induced by miR-345-3p inhibitors. MDA-MB-231 cells were transfected with miR-345-3p inhibitors for 48 h and treated with SC79 (4 μg/ml) for 30 min. The wound-healing efficacy were tested in MDA-MB-231 cells at 24 h. C, Akt activator SC79 abrogated the inhibition of cell proliferation abilities induced by miR-345-3p inhibitors. Relative cell viability of MDA-MB-231 cells were detected by CCK-8 kit at 24 h, 48 h, 72 h. D, Akt activator SC79 abrogated the inhibition of cell invasion abilities induced by miR-345-3p inhibitors. MDA-MB-231 cells invasion ability was measured by Transwell assay. All data are presented as the mean ± SD of triplicate experiments. The *P*-values < 0.05 were considered statistically significant. **P* < 0.05, ***P* < 0.01, ****P* < 0.001, *****P* < 0.0001.

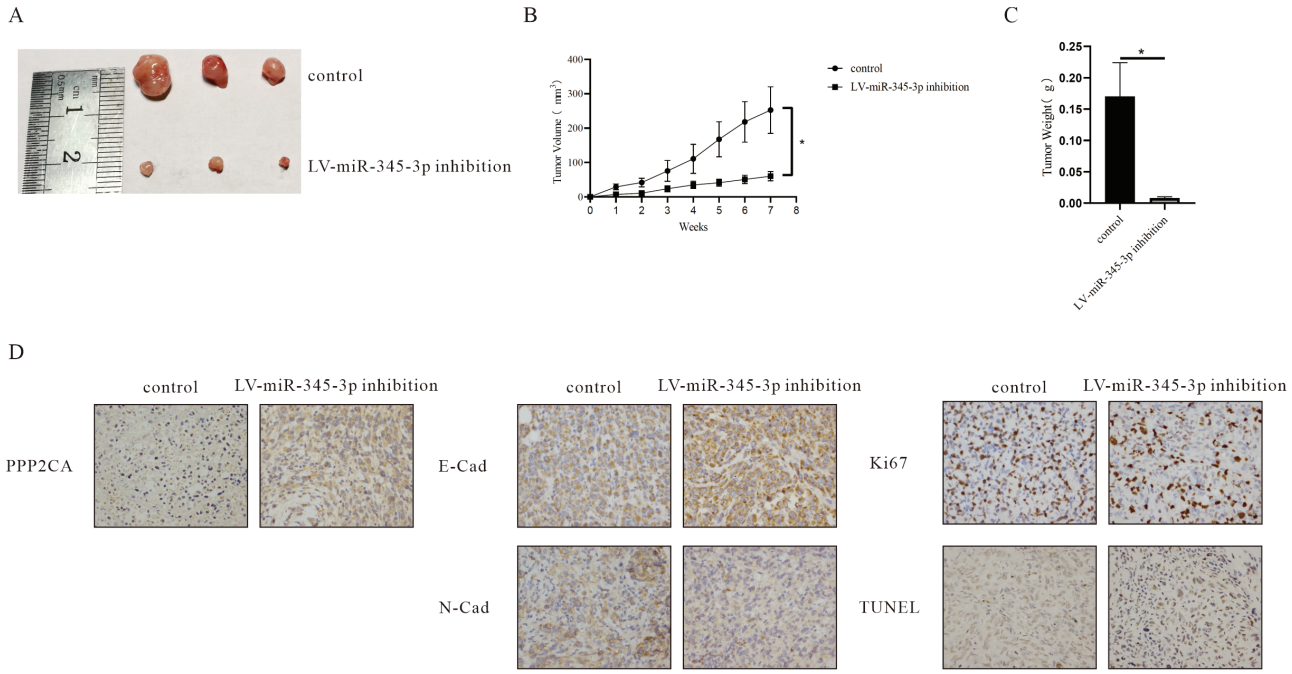

Figure 6. Knockdown of miR-345-3p attenuates cell growth and invasiveness *in vivo*. A, miR-345-3p knockdown obviously suppressed tumor growth compared with the control group. Representative images of the xenograft tumors in BALB/c-nude mice inoculated with the MDA-MB-231 control cells or stable miR-345-3p knockdown cells ($n = 3$ in each group). B, miR-345-3p knockdown obviously suppressed tumor growth compared with the control group. Tumor growth curves of MDA-MB-231 control cells or stable miR-345-3p knockdown cells in BALB/c-nude mice ($n = 3$ in each group). The volume of tumors was measured and calculated in indicated days. C, miR-345-3p knockdown obviously suppressed tumor growth compared with the control group. Tumor weight of BALB/c-nude mice implanted with the MDA-MB-231 control cells or stable miR-345-3p knockdown cells was measured at the end of the experiment ($n = 3$). D, Knockdown of miR-345-3p dramatically decreased proliferation and increased apoptosis *in vivo*. Immunohistochemical staining. Paraffin-embedded sections from the indicated xenograft tumor tissues were analyzed for PPP2CA, N-cadherin, E-cadherin, Ki67 and TUNEL by immunohistochemical staining ($n = 3$). All data are presented as the mean ± SD of triplicate experiments. The *P*-values < 0.05 were considered statistically significant. $^{*}P < 0.05$, $^{**}P < 0.01$, $^{***}P < 0.001$, $^{****}P < 0.0001$.

of miR-345-3p resulted in a significant increase in PPP2CA expression levels (Figure 6D). Additionally, further analysis of these tumor xenografts suggested that knockdown of miR-345-3p dramatically decreased proliferation and increased apoptosis (Figure 6D) as indicated with staining of Ki67 and TUNEL, respectively. Likewise, immunohistochemical analyses revealed that knockdown of miR-345-3p attenuates invasiveness as high E-cadherin expression and low N-cadherin were detected in tumor xenografts treated with miR-345-3p-inhibition lentivirus compared with the control group (Figure 6D). Collectively, these results indicated that knockdown of miR-345-3p suppressed breast cancer cell growth and invasiveness through upregulation of PPP2CA *in vivo*.

Discussion

Emerging evidence has indicated the important role of dysregulated miRNAs in the occurrence and development of cancer (11, 21, 22). Dysregulated miRNAs can function as either oncogenes or tumor suppressor by binding to their complementary target mRNAs, resulting in mRNA post-translation repression or degradation (7, 8). More importantly, miRNAs possess good stability in bodily fluids, such as urine, saliva and serum, and can be detected as novel noninvasive biomarkers for cancers (17, 22–24). Furthermore, selected miRNAs can targeted-regulate the expression of multiple mRNAs in disease conditions, which prompts miRNAs as a potential therapeutic target for clinical treatment (12, 25–27). In parallel, advances in RNA delivery technology make miRNA-based therapy possible (13, 28, 29).

Recent studies have highlighted the vital role of miR-345-3p in disease conditions. A previous study found that miR-345-3p exhibits protective effect on gestational diabetes mellitus through targeting TAK1 (19). Another study demonstrated that miR-345-3p suppressed oxidized low-density lipoprotein (oxLDL)-induced apoptosis and inflammation by targeting TRAF6 (18). However, the functional role of miR-345-3p in breast cancer is still unclear. Our results unveiled the molecular mechanisms how miR-345-3p was involved in the occurrence and development of breast cancer. In our study, we have demonstrated for the first time that miR-345-3p promotes proliferation and invasion of breast cancer cells by downregulating PPP2CA and activating PI3K-AKT signaling pathway. According to our results, miR-345-3p expression was significantly elevated in breast cancer tissues and breast cancer cell lines. More importantly, the expression of miR-345-3p was obviously upregulated in highly metastatic MDA-MB-231 and SKBR3 cells in comparison with low metastatic MCF-7 and T47D cells. These results suggest that miR-345-3p expression might be positively correlated with the metastatic ability of breast cancer cells. In addition, Kaplan-Meier plot demonstrated that breast cancer patients with higher expression of miR-345-3p had worse prognosis, indicating its oncogenic role in breast cancer. In this study, MCF-7 and MDA-MB-231 cells were transfected

with miR-345-3p mimics and miR-345-3p inhibitors respectively. MiR-345-3p mimics obviously promoted proliferation and invasion of breast cancer cells, while knockdown of miR-345-3p with the oligonucleotide inhibitor attenuated proliferation capacity and invasiveness in these breast cancer cells. Moreover, overexpression of miR-345-3p resulted in significant increase in the proliferation and invasion abilities of breast cancer cells by regulating expression of apoptosis and epithelial-mesenchymal transition (EMT)-related protein. Knockdown of miR-345-3p by miR-345-3p-inhibition lentivirus significantly suppressed breast cancer cell growth and invasiveness *in vivo*. Collectively, our findings imply that miR-345-3p might be an effective target for breast cancer treatment.

Another finding of our studies was that protein phosphatase 2 catalytic subunit alpha (PPP2CA) could be as a novel downstream target of miR-345-3p. PPP2CA is the catalytic subunit alpha of Protein phosphatase 2A (PP2A), a type of serine/threonine phosphatase involved in multiple cellular processes (30, 31). PP2A, as a confirmed tumor suppressor protein, was found to be altered or functionally inactivated in many cancers (32, 33). In addition, previous studies indicated that PPP2CA functioned as a suppressor of insulin's metabolic signaling pathway by inactivating the phosphorylation of AKT (34, 35). PI3K-AKT signaling pathway is one of the signaling pathways associated with insulin's metabolic signaling pathway. It is noteworthy that many investigations have reported the activation of PI3K-AKT signaling pathway in cancers (36–38). In our study, we identified PPP2CA as a direct downstream of miR-345-3p by taking advantage of bioinformatics strategies. Moreover, we verified the miR-345-3p-binding sites of PPP2CA by constructing luciferase vectors containing the wide-type and mutant binding sequence. Luciferase reporter assay indicated that miR-345-3p mimics significantly decreased the luciferase activity driven by PPP2CA 3′ UTR wide-type rather than PPP2CA 3′ UTR mutant. Consistent with these results, miR-345-3p mimics treatment obviously reduced the PPP2CA expressions at both mRNA and protein levels, while inhibition of miR-345-3p resulted in a remarkable increase in PPP2CA at mRNA and protein levels, suggesting that PPP2CA is the direct downstream target of miR-345-3p. Additionally, siRNA-mediated silencing of PPP2CA rescued the inhibition of cell proliferation and invasion induced by miR-345-3p inhibitors. Thus, these results indicate that PPP2CA play a crucial role in the regulation of miR-345-3p-mediated proliferation and invasion of breast cancer cells. In accordance with a previous study, our results shown that miR-345-3p activated PI3K-AKT signaling pathway through miR-345-3p-mediated suppression of PPP2CA and thus promoted proliferation and invasion of breast cancer cells (20).

In summary, we reported that miR-345-3p could promote proliferation and invasion of breast cancer cells by directly targeting PPP2CA, which could activate PI3K-AKT signaling pathway. All these findings highlight the significant role of miR-345-3p as well as PPP2CA in the progression of breast cancer, and provide a new target for the development of novel therapeutic strategies for breast cancer treatment in the future.

Supplementary material

Supplementary data are available at *Carcinogenesis* online.

Funding

National Natural Science Foundation of China (no. 81772844 and no. 82073255), Scientific and Technological Research Program of Chongqing Municipal Education Commission (grant number: KJQN202000450) and Graduate Scientific Research and Innovation Project of Chongqing (CYS20205).

Conflict of Interest Statement

There are no conflicts to declare.

References

1. Siegel, R.L. et al. (2021) Cancer statistics, 2021. *CA. Cancer J. Clin.*, 71, 7–33.
2. Kalimutho, M. et al. (2019) Patterns of genomic instability in breast cancer. *Trends Pharmacol. Sci.*, 40, 198–211.
3. Andre, F. et al. (2004) Breast cancer with synchronous metastases: trends in survival during a 14-year period. *J. Clin. Oncol.*, 22, 3302–3308.
4. Koboldt, DC et al. (2012) Comprehensive molecular portraits of human breast tumours. *Nature*, 490, 61–70.
5. Kozłowski, J. et al. (2015) Breast cancer metastasis—insight into selected molecular mechanisms of the phenomenon. *Postepy Hig. Med. Dosw. (Online)*, 69, 447–451.
6. Liang, Y. et al. (2020) Metastatic heterogeneity of breast cancer: molecular mechanism and potential therapeutic targets. *Semin. Cancer Biol.*, 60, 14–27.
7. Bartel, D.P. (2004) MicroRNAs: genomics, biogenesis, mechanism, and function. *Cell*, 116, 281–297.
8. Jafri, M.A. et al. (2017) Role of miRNAs in human cancer metastasis: implications for therapeutic intervention. *Semin. Cancer Biol.*, 44, 117–131.
9. Berezikov, E. (2011) Evolution of microRNA diversity and regulation in animals. *Nat. Rev. Genet.*, 12, 846–860.
10. Esquela-Kerscher, A. et al. (2006) Oncomirs—microRNAs with a role in cancer. *Nat. Rev. Cancer*, 6, 259–269.
11. Lee, Y.S. et al. (2009) MicroRNAs in cancer. *Annu. Rev. Pathol.*, 4, 199–227.
12. Rupaimoole, R. et al. (2016) miRNA Deregulation in cancer cells and the tumor microenvironment. *Cancer Discov.*, 6, 235–246.
13. Pecot, C.V. et al. (2013) Tumour angiogenesis regulation by the miR-200 family. *Nat. Commun.*, 4, 2427.
14. Yan, W. et al. (2018) Cancer-cell-secreted exosomal miR-105 promotes tumour growth through the MYC-dependent metabolic reprogramming of stromal cells. *Nat. Cell Biol.*, 20, 597–609.
15. Manterola, L. et al. (2014) A small noncoding RNA signature found in exosomes of GBM patient serum as a diagnostic tool. *Neuro. Oncol.*, 16, 520–527.
16. Schwarzenbach, H. et al. (2014) Clinical relevance of circulating cell-free microRNAs in cancer. *Nat. Rev. Clin. Oncol.*, 11, 145–156.
17. Mori, M.A. et al. (2019) Extracellular miRNAs: from biomarkers to mediators of physiology and disease. *Cell Metab.*, 30, 656–673.
18. Wei, Q. et al. (2020) MiR-345-3p attenuates apoptosis and inflammation caused by oxidized low-density lipoprotein by targeting TRAF6 via TAK1/p38/NF-kB signaling in endothelial cells. *Life Sci.*, 241, 117142.
19. Li,Y et al. (2021) miR-345-3p serves a protective role during gestational diabetes mellitus by targeting BAK1. *Exp. Ther. Med.*, 21, 2.
20. Bakirtzi, K. et al. (2011) Neurotensin signaling activates microRNAs-21 and -155 and Akt, promotes tumor growth in mice, and is increased in human colon tumors. *Gastroenterology*, 141, 1749–1761.e1.
21. Bertoli, G. et al. (2015) MicroRNAs: New biomarkers for diagnosis, prognosis, therapy prediction and therapeutic tools for breast cancer. *Theranostics*, 5, 1122–1143.

22. Hayes, J. et al. (2014) MicroRNAs in cancer: biomarkers, functions and therapy. *Trends Mol. Med.*, 20, 460–469.
23. Weber, J.A. et al. (2010) The microRNA spectrum in 12 body fluids. *Clin. Chem.*, 56, 1733–1741.
24. Grasedieck, S. et al. (2012) Impact of serum storage conditions on microRNA stability. *Leukemia*, 26, 2414–2416.
25. Iorio, M.V. et al. (2012) MicroRNA dysregulation in cancer: diagnostics, monitoring and therapeutics. A comprehensive review. *EMBO Mol. Med.*, 4, 143–159.
26. Li, Z. et al. (2014) Therapeutic targeting of microRNAs: current status and future challenges. *Nat. Rev. Drug Discov.*, 13, 622–638.
27. Bader, A.G. (2012) miR-34—a microRNA replacement therapy is headed to the clinic. *Front. Genet.*, 3, 120.
28. Trang, P. et al. (2011) Systemic delivery of tumor suppressor microRNA mimics using a neutral lipid emulsion inhibits lung tumors in mice. *Mol. Ther.*, 19, 1116–1122.
29. Ibrahim, A.F. et al. (2011) MicroRNA replacement therapy for miR-145 and miR-33a is efficacious in a model of colon carcinoma. *Cancer Res.*, 71, 5214–5224.
30. Sangodkar, J. et al. (2016) All roads lead to PP2A: exploiting the therapeutic potential of this phosphatase. *FEBS J.*, 283, 1004–1024.
31. Janssens, V. et al. (2001) Protein phosphatase 2A: a highly regulated family of serine/threonine phosphatases implicated in cell growth and signalling. *Biochem. J.*, 353(Pt 3), 417–439.
32. Westermarck, J. et al. (2008) Multiple pathways regulated by the tumor suppressor PP2A in transformation. *Trends Mol. Med.*, 14, 152–160.
33. Morita, K. et al. (2020) Allosteric activators of protein phosphatase 2A display broad antitumor activity mediated by dephosphorylation of MYBL2. *Cell*, 181, 702–715.e20.
34. Ugi, S. et al. (2004) Protein phosphatase 2A negatively regulates insulin's metabolic signaling pathway by inhibiting Akt (protein kinase B) activity in 3T3-L1 adipocytes. *Mol. Cell. Biol.*, 24, 8778–8789.
35. Resjö, S. et al. (2002) Protein phosphatase 2A is the main phosphatase involved in the regulation of protein kinase B in rat adipocytes. *Cell. Signal.*, 14, 231–238.
36. DeBerardinis, R.J. et al. (2008) The biology of cancer: metabolic reprogramming fuels cell growth and proliferation. *Cell Metab.*, 7, 11–20.
37. Fruman, D.A. et al. (2014) PI3K and cancer: lessons, challenges and opportunities. *Nat. Rev. Drug Discov.*, 13, 140–156.
38. Hirsch, E. et al. (2014) PI3K in cancer-stroma interactions: bad in seed and ugly in soil. *Oncogene*, 33, 3083–3090.